A Nested Wideband Adaptive Array Using Multirate Filter Banks

*Choo Leng Koh and Stephan Weiss**
Communications Research Group, School of Electronics & Computer Science
University of Southampton, Southampton SO17 1BJ, UK,
Tel: +44 (0)23 8059 2422;
e-mail: clk02r@ecs.soton.ac.uk, sw1@ecs.soton.ac.uk

ABSTRACT

In this paper, we derived a generalised subband based scaled aperture (SSA) beamformer, exemplarily for the generalised sidelobe canceller (GSC). This structure is useful for broadband beamforming where near-constant spatial resolution over a wide range of frequencies is desired. The generalised SSA beamformer decomposes broadband signal into subbands, which are grouped into octave intervals. By drawing inputs from sensors with a wider aperture for lower octave bands, an octave-invariant resolution is achieved. We demonstrate that the SSA operates well across octave boundaries and additionally can benefit from an increase performance and reduced complexity when compared to similar subband and fullband domain beamforming structures.

1 INTRODUCTION

Broadband beamforming using a linear uniformly spaced array results in a frequency dependent spatial resolution, since the later is proportionally related to both the array's aperture and the frequency of the target signal. Hence for an array with fixed aperture, the spatial resolution decreases with frequency. In order to limit the variation in spatial resolution, recommendations have been made to limit the processing of signals to an octave [1]. To overcome the octave barrier, the used of unequally spaced sensor arrays [2, 3], implementation of harmonic nesting structure [4, 5] and a technique based on approximating the ideal continuous aperture [6] have been suggested.

Based on a harmonically nested array with a scaling in aperture for different octave frequency intervals [4, 5, 7], this paper discusses a generic adaptive subband based broadband beamformer having scaled aperture. Decomposing broadband sensor signals into decimated frequency bands ("subbands") is advantageous in terms of reducing the computational complexity and additionally increasing the convergence speed of LMS-type adaptive beamforming algorithms [8]. Further, in this paper we discuss how the subband approach can be exploited to form octave groups of subbands, which draw their inputs from sensor sets of different spacing and aperture as a generalisation of [4, 9].

In the following, we review the subband based broadband beamforming approach in Sec. 2. Sec. 3 introduces the proposed subband scaled aperture beamformer which will be simulated and compared to standard schemes in Sec. 5. Conclusions are drawn in Sec. 6. In our notation, we use lowercase and uppercase boldface characters to denote vector and matrix quantities, respectively.

2 SUBBAND BASED BEAMFORMING

2.1 LCMV Broadband Beamforming

Exemplarily for a broadband beamformer, we here utilise a linearly constrained minimum variance (LCMV) approach [10], which can be efficiently implemented by means of a generalised sidelobe canceller (GSC) [11]. The LCMV problem for optimising array weights can be formulated as $\mathbf{w} = \arg\min_{\mathbf{w}} \mathbf{w}^H \mathbf{R}_{xx} \mathbf{w}$ subject to $\mathbf{C}^H \mathbf{w} = \mathbf{f}$, where $\mathbf{w}$ contains the filter coefficients and $\mathbf{R}_{xx}$ is the covariance matrix of the observed array data. The constraint matrix $\mathbf{C}$ and the constraining vector $\mathbf{f}$ impose linear constraints, such as the preservation of a signal of interest impinging onto the array from a specific direction of arrival (DOA). The GSC performs a projection of the data onto the unconstrained subspace, where standard unconstrained optimisation algorithms such as the least mean squares (LMS) or recursive least square (RLS) algorithms [12] can be deployed.

2.2 Subband Decomposition

Subband based beamforming requires filter banks to decompose the broadband sensor signals by means of analysis filter banks into K different frequency bands, which can be operated at an N times lower sampling rate due to their reduced bandwidth. However, for critical decimation, $N = K$, spectral aliasing limits the performance of any processing in the subband domain, which can be mitigated by taking inter-subband correlations explicitly into accounts when designing subband based algo-

*This work was supported through the UK MoD's Corporate Research Programme.

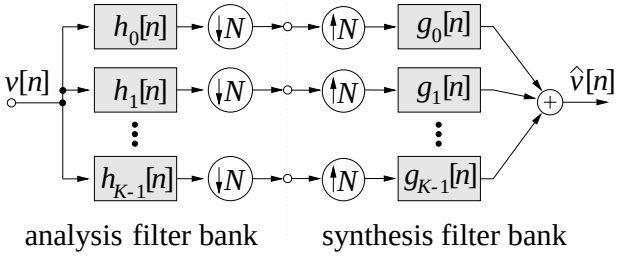

Figure 1: Subband decomposition by mean of analysis and synthesis filter banks.

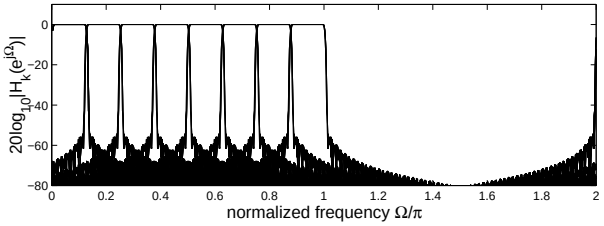

Figure 2: Filter bank characteristic for $K = 16$ and $N = 14$ based on a prototype with $L_p = 448$ coefficients.

rithms [13]. A simpler approach is to oversample subbands, i.e. decimate by a factor of $N < K$ [14], which can efficiently suppress aliasing in subbands and permit subbands to be processed independently.

Subband decompositions are performed by analysis filter banks such as shown in Fig. 1, consisting of a series of analysis filters $h_k[n]$, $k = 0(1)K-1$, and decimation by a factor N. Synthesis is achieved by upsampling by a factor of N followed by appropriate interpolation filters $g_k[n]$. For oversampled filter banks (OSFBs) with $N < K$, which are considered here, the filters $h_k[n]$ and $g_k[n]$ can be efficiently designed and implemented based on the modulation of a single prototype lowpass filter. In our work, we employ the generalised discrete Fourier transform (GDFT) for modulation, which admits a straightforward design according to [16]. As an example, the magnitude characteristics for $H_k(e^{j\Omega}) \circ\!\!-\!\!\bullet\, h_k[n]$ of an OSFB with $K = 16$ and $N = 14$ using a filter length of $L_p = 448$ coefficients is given in Fig. 2. Note that the resulting subband signals are complex valued, and that for real valued array signals the shown $K/2 = 8$ subbands are complex conjugate versions of the remaining bands, which are therefore redundant and can be omitted from processing.

2.3 Subband Beamformer

The block diagram of a standard subband beamformer processing fixed aperture array data is shown in Fig. 3 [8, 17]. The analysis OSFBs, labelled **A**, decompose the broadband array signals into subbands. Within each subband, an independent broadband beamformer, here exemplarily a GSC, is operated. The beamformer

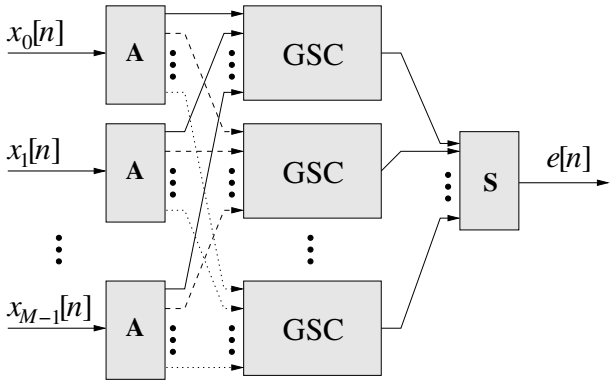

Figure 3: Subband adaptive beamformer with fixed aperture.

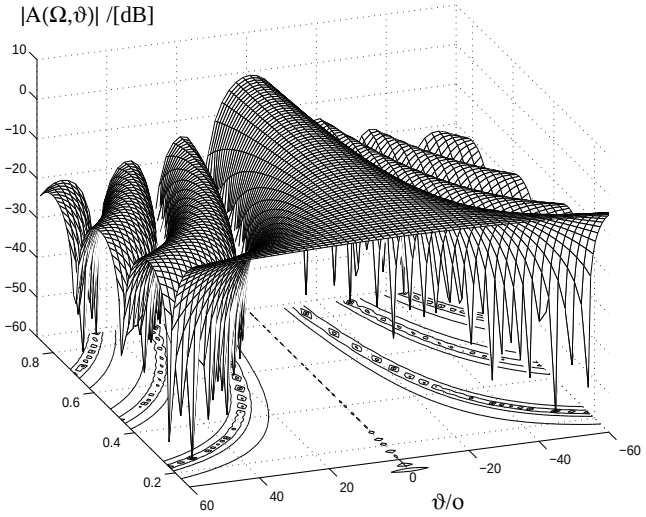

Figure 4: Directivity pattern of beamformer with fixed aperture.

outputs form the basis of a reconstructed fullband beamformer output by means of a synthesis OSFB denoted as **S**.

The spatial resolution is reciprocally proportional to both aperture and the frequency of the impinging waveform. As such, for the beamforming structure in Fig. 3, poor resolution is encountered at the lower frequencies. This effect is indicated by the directivity pattern $|A(\Omega, \vartheta)|$, recording the beamformer's gain in dependency of the normalised angular frequency Ω and a DOA ϑ, in Fig. 4, which demonstrates a beamformer's gain response as a function of frequency and DOA. To overcome this, the subband based scaled aperture beamformer is introduced.

3 GENERALISED SUBBAND BASED SCALED APERTURE BEAMFORMER

The subband based scaled aperture (SSA) approach uses a different array aperture within each octave, i.e. progressively lower frequency octaves are processed by pro-

gressively wider arrays. In doing so, a constant spatial resolution is maintained from octave to octave [4, 9]. We commence with an example in Sec. 3.1, and generalise the structure in Sec. 3.2

3.1 Example

An example of the proposed structure for an array operating over a range of $F = 3$ octaves utilising $M = 4$ sensors per octave is provided in Fig. 5. These octaves can be resolved by splitting a broadband signal into $K = 8$ uniform subbands. Discarding the DC component in subband #0, the lowest frequency octave is contained in subband #1, while subbands #2 and #3 hold the second octave and the highest frequency octave spans subbands #4 to #7. In order to enhance spatial resolution, the array aperture is doubled when one from the higher octave goes to the next-lower one [9]. In Fig. 5, the subband GSC beamformer #1 operates on the lowest band and draws its input from the largest aperture. The GSC processors #2 and #3 operate on the next higher octave, with the remaining 4 processors responsible for the highest octave band covering 4 subbands. The aperture size for the three octave bands are $D = 3d$, $D = 6d$ and $D = 12d$ respectively, with d being the distance between adjacent sensors satisfying the criteria to avoid spatial aliasing for the smallest wavelength.

The use of nested arrays such as shown in Fig. 5 is economical, since sensors can be reused and be part of several sub-arrays, such as the sensor signals $x_0[n]$, $x_2[n]$ and $x_4[n]$ in the above example, which requires a total of $M_{\text{total}} = 8$ nested array elements. If these sensor positions were extracted from a linear uniformly spaced array, it would contain $M_{\text{uniform}} = 13$ such elements before thinning.

3.2 Generalisation

As a generalisation of the above example, it can be shown that the sensor signals need to be decomposed into

$$K = 2^F \ . \tag{1}$$

uniform subbands in order to set up a subband beamformer which can resolve F octaves. Further, the generalisations for M_{total} and M_{uniform} can be shown to obey

$$M_{\text{uniform}} = M + \left[(M-1)(2^{(F-1)} - 1)\right] \ , \tag{2}$$

and

$$M_{\text{total}} = \lfloor (\frac{M}{2}) \rfloor (F+1) + \text{mod}_2(\text{M}) \ , \tag{3}$$

where $\lfloor \cdot \rfloor$ is the floor operator and mod_n represents the modulo-n operation. With (2) and (3), we can design an SSA for any number of octaves F and sensor elements M per octave. Note that the K stated in (1) is the minimum number of subbands required to resolve the desired number of octaves; employing an integer multiple of this K is permissible and may have advantages in terms of algorithmic complexity and convergence speed of an adaptive algorithm.

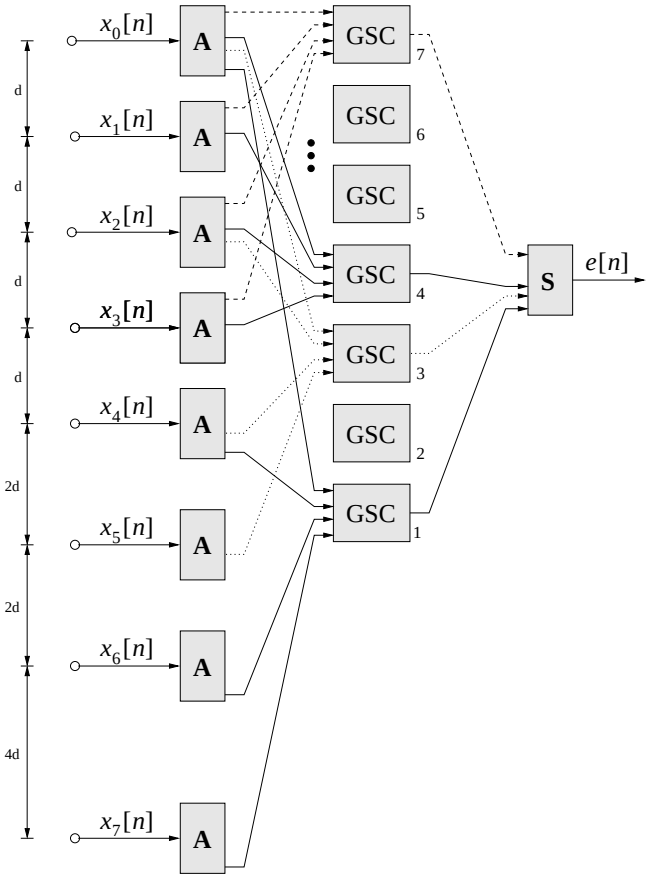

Figure 5: Subband adaptive beamformer with scaled aperture.

4 COMPUTATIONAL COMPLEXITY

4.1 Fullband Cases

A fullband fixed aperture beamformer employing a GSC driven by a normalised least mean square (NLMS) algorithm requires a computational complexity of $(ML)^2$ multiply accumulate (MAC) operations for its blocking matrix and quiescent vector and $3ML+3M$ for its adaptive part, with L representing the temporal dimension — i.e. the tap delay line length — of the beamformer. This accrues to

$$C_{\text{fb,fixed}} = (ML)^2 + 3ML + 3M \tag{4}$$

If we used a nested array and utilise all available sensor signal to operate a fullband GSC,

$$C_{\text{fb,nested}} = (M_{\text{total}}L)^2 + 3M_{\text{total}}L + 3M_{\text{total}} \tag{5}$$

would result, with M_{total} according to (3).

4.2 Subband Cases

For a subband decomposition, an efficient modulated OSFB analysis or synthesis filter bank is associated with $C_{\text{bank}} = \frac{1}{N}(4K \log_2 K + 4K + L_p)$, with L_p being the length of the prototype filter [15]. Therefore a fixed

aperture subband beamformer causes extra computational complexity in the form of $(M+1)$ filter banks for decomposition and subsequently reconstruction of signals according to Fig. 3. Computational savings arise in the subband domain due to an N times lower update rate and an approximately N times shorter temporal dimension required for any beamformer, although now K parallel realisations have to be operated [8]. There, the cost of a fixed aperture subband beamformer can be denoted as approximately

$$C_{\text{sb,fixed}} = \frac{K}{N}\left[(M\frac{L}{N})^2 + 3M\frac{L}{N}\right] + (M+1)\cdot C_{\text{bank}} \quad (6)$$

For the proposed SSA beamformer, the number of active sensor signals per octave is not changed compared to the fixed aperture scheme, but a higher number of analysis filter banks has to be implemented according to Fig. 5, resulting in

$$C_{\text{sb,nested}} = \frac{K}{N}\left[(M\frac{L}{N})^2 + 3M\frac{L}{N}\right] + (M_{\text{total}}+1)\cdot C_{\text{bank}} \quad (7)$$

MACs per fullband sampling period.

5 SIMULATIONS AND RESULTS

In the following, we assess and compare the proposed SSA broadband beamformer in terms of the achieved directivity pattern and its octave-invariant resolution, in terms of interference suppression and convergence, and in terms of complexity to other fullband and subband schemes drawing their inputs from sensors with a fixed aperture.

5.1 Directivity Pattern

The flexibility of the SSA beamformer for various sensor element numbers M and octaves F is illustrated in Fig. 6 by the example of $M = 11$ and $F = 4$, requiring a decomposition into $K = 16$ subbands. Comparing the shown directivity pattern with Fig. 4, a significant improvement in maintaining octave-invariant and therefore near frequency-invariant resolution across a wide spectrum can be noted.

The SSA beamformer with adaptive filters incorporated enables to steer nulls towards interferers illuminating the array from directions other than the look direction. To demonstrate this effect, we apply two broadband interferers impinging onto the array from angles of $-30°$ and $10°$ respectively, while the signal of interest lies at broadside. The simulation utilises $F = 3$ octaves with $M = 11$ sensors per octave and subsequently $K = 16$. The filter banks are the ones characterised in Fig. 2, based on a prototype of length $L + p = 448$ permitting a decimation factor of $N = 14$. After adaptation, the directivity pattern in Fig. 7 illustrates the successful nulling of the two broadband interferers. This contrasts with Fig. 6, where no adaptation is applied and subsequently the quiescent beam pattern is not set to suppress any specific interferers.

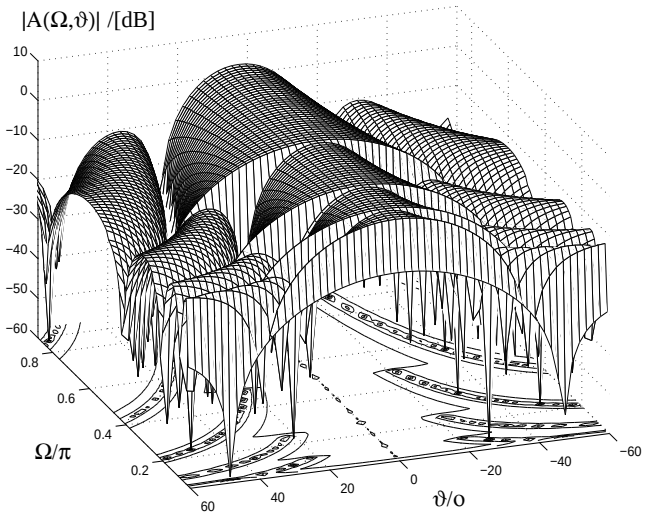

Figure 6: Directivity pattern of subband beamformer with scaled aperture $M = 11$, $F = 4$.

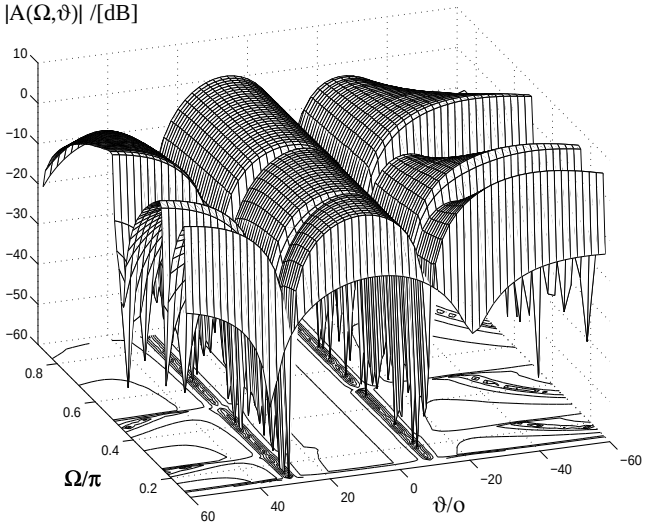

Figure 7: Directivity pattern of SSA beamformer in the presence of broadband interferers from $-30°$ and $10°$.

5.2 Interference Suppression and Signal Distortion

A performance comparison between subband scaled aperture, subband fixed aperture and fullband fixed aperture in term of the mean squared residual error is carried out. The residual error here is defined as difference between the beamformer output $e[n]$ in Figs. 3 and 5 and the signal of interest from broadside. Therefore any remaining interference and noise as well as any distortion imposed on the signal of interest is measured. In the simulated scenario, the signal of interest is at the array's broadside, while broadband interferers impinge form $-20°$ at an SIR of -40 dB, corrupted by uncorrelated noise at 10 dB SNR. The beamformers draw their inputs from $M = 5$ sensors in the fixed aperture case,

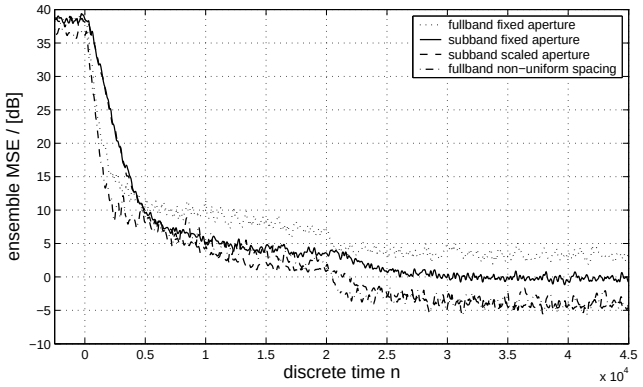

Figure 8: Learning curves.

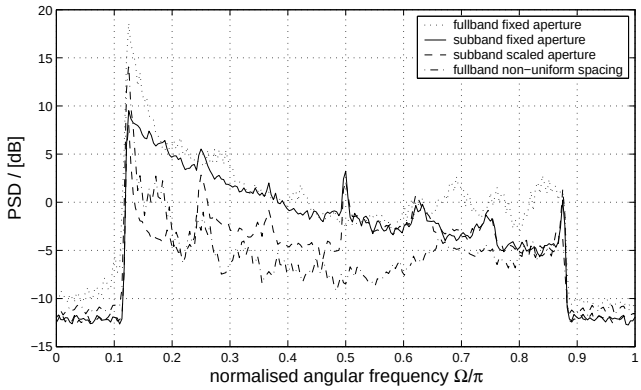

Figure 9: PSD of residual error at steady state.

and $M_{\text{total}} = 9$ sensors in the nested array case.

The fullband beamformer represents a traditional time domain implementation where no decomposition of the broadband signal is carried out. It is either applied to $M = 5$ uniformly spaced array elements, or alternatively utilises all M_{total} input, and applies a tap delay line of $L = 64$ to each sensor signal. The subband beamformers use $K = 16$ channel filter banks with $N = 14$ and prototype length $L_p = 448$ as characterised in Fig. 2. The temporal dimension of the subband based beamformer is shortened accordingly. In all cases, the GSC is operated in combination with an NLMS algorithm [12]. The adaption of the beamformers starts at $n = 0$ with a step-size of $\mu = 0.5$, and at $n = 20000$ the step-size is reduced by a magnitude of 10.

Learning curves depicted in Fig. 8 indicate that the SSA outperforms the fixed aperture subband based beamformer in having faster convergence speed and lower steady state error. The latter is due to an enhanced suppression of interferers at low frequencies, where the increased spatial resolution is of benefit. Surprisingly, the steady-state MSE performance is the same as the fullband algorithm exploiting all M_{total} sensors, which is however reached at a substantially lower complexity.

To further analysis the characteristic of the beamformers, power spectral densities (PSD) of the various steady-state errors are presented in Fig. 9. The fullband fixed aperture having $M = 5$ sensors exhibits high power at lower frequencies, trailing off as frequency increases. The subband fixed aperture scheme has similar PSD characteristic to the fullband albeit a sightly lower PSD at lower frequencies. This corresponds to the directivity pattern in Fig 3, where the larger beamwidth at lower frequencies allows more signal power to pass through the system. As the beamwidth narrows towards the higher frequencies, better resolution is observed. The proposed SSA approach gives a fairly octave-invariant PSD due to different aperture sizes. The octave structure is clearly visible in Fig. 9, where lower interference suppression can be seen at the lower frequencies within each octave.

Fig. 10 shows the gain response of the SSA beamformer from broadside. This figure indicates that the 0 dB constraint towards broadside is fulfilled and that the ripple of the beamformer gain is fairly small despite the subband edges and the integration of various apertures within the beamformer. This also highlights that peaks in the PSD of the subband approaches in Fig. 9 are not due to distortion effects at the octave margins but are a result of slow convergence at the band edges of individual subbands caused by low input power to the adaptive algorithm [18].

5.3 Complexity

For the scenario in Sec. 5.2 with $M = 5$ and $F = 3$, $M_{\text{total}} = 9$, $K = 16$, $N = 14$, and $L_p = 448$ for the proposed SSA scheme, the arising computational complexities are given in Fig. 11. The SSA beamformer requires an extra 4 sensors inputs and hence 4 more analysis filter bank operations compared to the subband fixed aperture architecture. Note that the computational complexity of the subband schemes in general is significantly lower than the fullband approach. For the

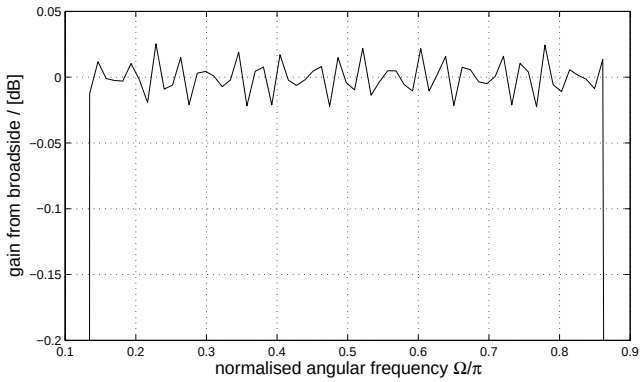

Figure 10: Gain response of the SSA beamformer toward broadside representing the distortion imposed on the signal of interest.

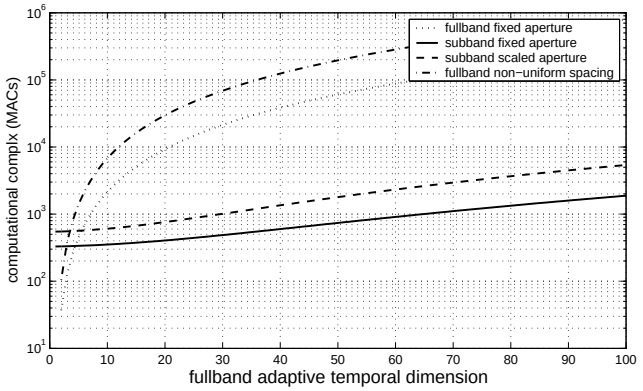

Figure 11: Computational complexities of fullband fixed aperture, subband fixed aperture and subband scaled aperture.

simulations in Sec. 5.2, where SSA and a fullband nested array beamformer utilising all $M_{\text{total}} = 9$ sensor signals provided a similar steady-state performance in terms of interference suppression, it can be noted that the computational complexity differs by 2 orders of magnitude.

6 CONCLUSIONS

We have proposed a subband based scaled aperture beamformer which has the ability to maintain approximately constant resolution across a wide frequency range. Poor resolution encountered by fixed aperture beamformers at low frequencies can be overcome by drawing sensor inputs from a nested array, such that lower octaves correspond to an array of increased aperture. We have shown that the constraint is fulfilled across the octave band margins, and only limited by the filter bank's distortion function, which can be kept as small as necessary by design.

Additionally, the SSA scheme inherits the low computational complexity of general subband approaches. We have compared various broadband beamforming implementation in both the fullband and subband domain, whereby the SSA does not suffer any degradation with respect to the MSE performance when compared to a fullband scheme exploiting the entire sensor array data albeit at a much higher cost.

REFERENCES

[1] D. Nunn, "Suboptimal Frequency-Domain Adaptive Antenna Processing Algorithm for Broad-Band Environments," *IEE Proc. F: Radar & Sig. Proc.*, **134**(4): 341–351, 1987.

[2] J. H. Doles and F. D. Benedict, "Broad-band array design using the asymptotic theory of unequally spaced arrays," *IEEE Trans. Ant. Prop.*, **36**(1): 27–33, 1988.

[3] A. Ishimaru, "Theory of unequally-spaced arrays," *IEEE Trans. Ant. Prop.*, **10**(6): 691–702, 1962.

[4] W. Kellermann, "A self-steering digital microphone array," in *Proc. IEEE ICASSP*, Toronto, Ont., Canada, 1991, 5, 3581–3584.

[5] T. Chou, "Frequency-independent beamformer with low response error," in *Proc. IEEE ICASSP*, Detroit, Michigan, 1995, 5, 2995–2998.

[6] D. B. Ward, R. A. Kennedy, and R.C. Williamson, "Theory and design of broadband sensor arrays with frequency invariant far-field beam patterns," *J. Acoustic Society of America*, **97**(2), 1023–1034, 1995.

[7] H. L. Van Trees, *Optimum Array Processing*, Wiley, New York, 2002.

[8] S. Weiss, R. W. Stewart, M. Schabert, I. K. Proudler, and M. W. Hoffman, "An Efficient Scheme for Broadband Adaptive Beamforming," in *Proc. Asilomar Conf. Sig. Sys. and Comp.*, Monterey, CA, 1999, 1, 496–500.

[9] S. Weiss, R. W. Stewart, and W. Liu, "A broadband adaptive beamformer in subbands with scaled aperture," in *Proc. Asilomar Conf. Sig. Sys. and Comp.*, Monterey, CA, 2002, 2, 1298–1302.

[10] O. L. Frost, III, "An Algorithm for Linearly Constrained Adaptive Array Processing," *Proceedings of the IEEE*, **60**(8), 926–935, 1972.

[11] L. J. Griffith and C. W. Jim, "An Alternative Approach to Linearly Constrained Adaptive Beamforming," *IEEE Trans. Ant. Prop.*, **30**(1), 27–34, 1982.

[12] B. Widrow and S. D. Stearns, *Adaptive Signal Processing*, Prentice Hall, Englewood Cliffs, New York, 1985.

[13] A. Gilloire and M. Vetterli, "Adaptive Filtering in Subbands with Critical Sampling: Analysis, Experiments and Applications to Acoustic Echo Cancelation," *IEEE Trans. Sig. Proc.*, **40**(8), pp. 1862–1875, 1992.

[14] W. Kellermann, "Analysis and design of multirate systems for cancellation of acoustical echoes," in *Proc. IEEE ICASSP*, New York, USA, 1988, 5, pp. 2570–2573.

[15] S. Weiss. "Analysis and Fast Implementation of Oversampled Modulated Filter Banks". In J. G. McWhirter and I. K. Proudler, editors, *Mathematics in Signal Processing V*, chapter 23, pages 263–274. Oxford University Press, March 2002.

[16] M. Harteneck, S. Weiss, and R. W. Stewart, "Design of Near Perfect Reconstruction Oversampled Filter Banks for Subband Adaptive Filters," *IEEE Trans. on Circuits & Systems II*, **46**(8), pp. 1081–1086, 1999.

[17] W. H. Neo and B. Farhang-Boroujeny. Robust Microphone Arrays Using Subband Adaptive Filters. *IEE Proceedings — Vision, Image, and Signal Processing*, 149(1):17–25, Feb. 2002.

[18] D. R. Morgan. Slow Asymptotic Convergence of LMS Acoustic Echo Cancellers. *IEEE Transactions on Speech and Audio Processing*, 2(3):126–136, March 1995.